Post-installed shear reinforcement for concrete thick slabs

Mathieu Fiset

Centre de recherche sur les infrastructures en béton (CRIB),
Université Laval,
1065 Avenue de la médecine, Québec (Québec), G1V-0A6, Canada
Supervisors: Josée Bastien and Denis Mitchell

Abstract
Many concrete bridges may be associated to a simple thick slabs structural system. With the increase in traffic loads and material degradation, some of these structures need to be strengthened in shear. The goal of this research is to study the behaviour of slabs strengthened with post-installed shear reinforcement and to provide an analytical method of design. The studied reinforcement methods consist in installing rebars into pre-drilled holes in the slab with different anchor systems. The first experimental results showed that shear-strengthened slabs can have failure loads 46% higher than an unstrengthened slab but 29% lower than the Canadian code prediction for conventional stirrups. The VecTor2 finite element analysis tool will be used to study the parameters influencing the slabs behaviour. The first experimental results and associated numerical models outcomes will be presented.

1 Introduction

For simple structural systems such as thick slab bridges, it was commonly assumed that the concrete was able to resist shear stresses and that stirrups were therefore not required. However, due to the increase in traffic loads and material degradation, nowadays some of these thick slabs need to be strengthened in shear. In the past, shear strengthening methods have been examined and tested on beams. Among them, the addition of near surface mounted rods [1] and the addition of external carbon fiber reinforced polymer laminates [2,3] have been suggested. Although these methods can be effective on beams, the fact that the reinforcement is installed on either side of the concrete section raised the question of their effectiveness on the full width of large elements as slabs. More recently, the use of vertical rods anchored into thin slabs with epoxy adhesive to resist punching shear has proven to give good results [4]. However, very few studies were performed on thick slabs where the size effect can become important with regards to shear performance. Therefore, improved knowledge on shear strengthening methods for thick slabs through laboratory testing and numerical means has gained wide interest.

In the present paper, the strengthening methods under investigation consist in steel rebars introduced into pre-drilled holes with different anchor systems: epoxy adhesive, internal and external mechanical anchorage. Two series of tests performed on deep beams (slices of slabs) were conducted up to shear failure [5,6]. The first set of results showed that while shear-strengthened slabs can exhibit failure loads 46% higher compared with the ones of unstrengthened slabs, they showed failure loads 29% lower than the Canadian code prediction values [7] related to conventional shear reinforcement (stirrups). One of the main objectives of the underway research is to adequately predict the increase in shear strength of thick slabs strengthened by various methods and to provide basis for a normative strengthening design method in light of the experimental and numerical results. To achieve this, the proposed finite element models should be able to reproduce the behaviour of the tested beams. Once this is achieved, these models will help to perform parametric analysis to study the most important parameters influencing the slabs behaviour. The finite element analysis tool, VecTor2, will be used herein to study the influence of the relative rigidity of components, material properties and type of post-installed reinforcements including their anchorage and geometry. Some of the studied anchorage systems exhibited slippage during loading, a phenomena which should be taken into account by the numerical models.

Proc. of the 9th *fib* International PhD Symposium in Civil Engineering, July 22 to 25, 2012,
Karlsruhe Institute of Technology (KIT), Germany, H. S. Müller, M. Haist, F. Acosta (Eds.),
KIT Scientific Publishing, Karlsruhe, Germany, ISBN 978-3-86644-858-2

2 Review of experimental beams tests

Experimental tests were performed on two (2) series of beams (slices of slab), identified as the PP and BC series. The dimensional properties and strengthening rebar arrangements of the tested beams are summarized in Table 1 and Figure 1. For both series, each beam had a 4 meters free span, a 610mm width "b" and was designed to allow shear failure.

Table 1 Details of reinforced beams

Beam	Anchor	h [mm]	d [mm]	a/d	ρ [%]	s [mm]	s/d_v	A_v [mm²]	f_c [MPa]	E_c [MPa]
PP1	Epoxy	450	370	3.60	3.10	240	0.72	400	32.5	28 382
PP2	Epoxy	450	398	3.35	2.06	260	0.73	200	35.2	30 580
PP3	Epoxy	750	698	2.87	1.17	470	0.75	400	35.0	29 395
BC1	Stirrups	750	694	2.88	1.65	380	0.61	400	33.3	25 704
BC2	Epoxy	750	694	2.88	1.65	380	0.61	400	34.5	26 315
BC3	Epoxy	750	694	2.88	1.65	380	0.61	400	32.6	25 029
BC4	HSLG	750	694	2.88	1.65	380	0.61	292	31.5	24 144
BC5	Bolt	750	694	2.88	1.65	1000	1.60	1290	31.2	25 333

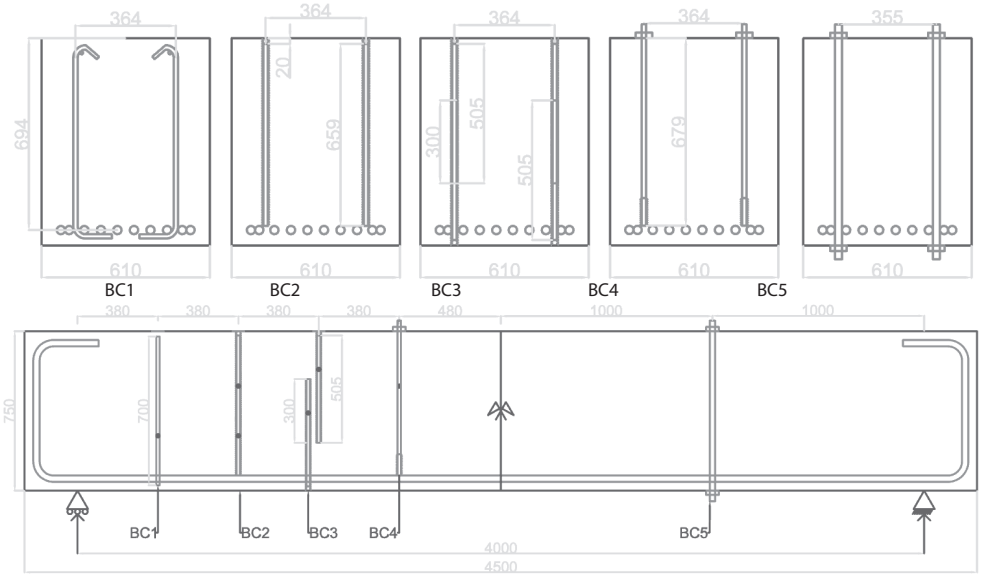

Fig.1 Specimens of BC series.

For all 3 PP beam categories (PP1, PP2 and PP3), 2 unstrengthened beams and 2 strengthened beams with the same overall dimensions were tested. In these PP series, the shear strengthening method consists in vertical post-installed rebars introduced into pre-drilled holes at specific locations along the beams and anchored by epoxy adhesive. This method is similar to that of the beam BC2 illustrated at Figure 1. The PP1 and PP3 specimens were strengthened with 2-15M rebars and PP2 specimens with 2-10M rebars respectively. The chosen spacing ratio of rebars, s/d_v, is close to the maximum value of 0.75 allowed by Canadian standards for conventional stirrups. While all specimen where simply supported, the PP1 and PP2 specimens were loaded at one-third of their span, whereas the PP3 specimens were loaded at mid-span.

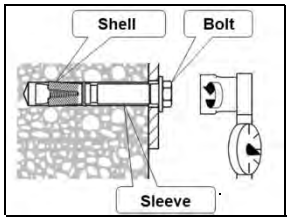

Fig.2 HSLG anchor used for BC4

The BC series differs from the PP series in terms of reinforcement ratios, transverse reinforcement spacing and strengthening methods. The BC1 specimen had stirrups as prescribed by Canadian standards and therefore was the only specimen of the BC series reinforced in shear before concrete casting. Similar to the PP3 specimens, the BC2 and BC3 specimens were strengthened with post-install 15M rebars anchored with epoxy adhesive into pre-drilled holes. The BC3 specimen has the particularity that its rebars overlap at mid height of the beam, over 300mm. The BC4 specimen was strengthened with vertical rebars inserted into pre-drilled holes from the top of the beam down to the location of the longitudinal rebars. The shear reinforcement is restrained with an anchor plate on the top face of the beam and with a mechanical anchorage at the bottom of the vertical rebars (Fig. 2). When opened, the shell of the mechanical anchorage exerts lateral pressure on the internal surfaces of the hole, which produces a frictional force and anchors the rebar. The BC5 specimen was strengthened with one pair of high strength bars inserted in pre-drilled holes and anchored on both top and bottom faces of the beam with an anchor plate. Each of the 5 BC beams were loaded at their mid span up to failure. Once a side of the beam reached its ultimate loading, this side of the specimen was strengthened in shear with external stirrups (Dywidag bars) and the beam was reloaded in order to reach the ultimate load of the specimen's other side.

2.1 Materials

The concrete mechanical properties presented in Table 1 were obtained according to standards ASTM-C39 and ASTM-C469. According to ASTM E08-04 and ASTM E111-04, the yield strength F_y, the ultimate strength F_u and the Young modulus E_s of the rebars were 472MPa, 660MPa and 178GPa respectively. The associate hardening strain was 23 mm/m and the ultimate strain was 114 mm/m. As specified by the manufacturer, the yield and the ultimate strength of the high strength steel bars of the beam BC4 were 642MPa and 800MPa, respectively. The maximum load for the expansive mechanical anchor was 84.5kN. The yield strength and the ultimate strength of the Dywidag bars used for the external shear strenthening of beam BC5 beam were 517MPa and 689MPa, respectively. A commercially available epoxy adhesive was used for all PP beam series as well as for beams BC1, BC2 and BC3. As specified by the manufacturer, the epoxy adhesive mechanical properties were: 12.4MPa bond strength (ASTM C882-91), 82.7MPa compressive strength (ASTM D-695-96), 1493MPa compressive modulus (ASTM D-695-96), 43.5MPa tensile strength and 2% elongation at failure (ASTM D-638-97).

3 Numerical model

The finite element numerical portion of the study is still underway. Up to now, the Vector2 numerical tool was used. This finite element software was developed at the University of Toronto for the analysis of two dimensional finite element models of concrete structures with rotating smeared crack. The analyses are based on the modified compression field theory (MCFT) [8] and disturbed stress field model (DSFM) [9]. With VecTor2, many options are available to model the material's behaviour. The basic options were initially selected. Therefore the steel behaviour is associated to a trilinear law as shown in Figure 3. For the tension behaviour of concrete, the σ-ε law is linear up to the tensile strength. Beyond this point, the tension softening effect is represented with a bilinear law. The tension stiffening effect is also included according to the model of Lee [10]. In compression, the cracked concrete behaviour includes compression softening effects and is modelled with equation (1).

As shown in Figure 4, the beam BC1 was modelled with 2D membrane elements. Because of the symmetry of the geometry and loading, half of the beam was modelled. Boundary conditions are imposed as follows, X displacements are blocked at mid-span and Y displacements are blocked at

support. The supports and the loading plate surface were modelled to best represent the laboratory conditions. For the beam BC1, the longitudinal rebars and the stirrups were modelled with truss elements perfectly linked with the nodes of the finite element mesh. For the beams with epoxy adhesive, link elements (spring) may be used to model the potential slippage of the shear reinforcements.

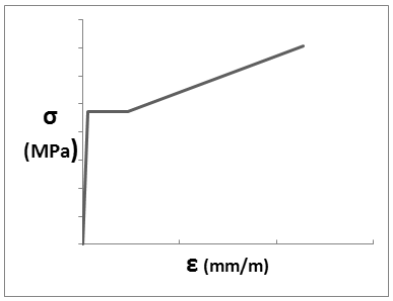

Fig.3 Behaviour of steel

$$f_{c2} = -f_p\left[2\left(\frac{\varepsilon_{ci}}{\varepsilon_p}\right) - \left(\frac{\varepsilon_{ci}}{\varepsilon_p}\right)^2\right] \quad (1)$$

Where:

$$f_p = \beta_d f_c^{'} \quad (2)$$

$$\varepsilon_p = \beta_d \varepsilon_c^{'} \quad (3)$$

$$\beta_d = \frac{1}{1+0.55C_d} \quad (4)$$

$$C_d = \begin{cases} 0 & \text{if } r < 0.28 \\ 0.35(r-0.28)^{0.8} & \text{if } r > 0.28 \end{cases} \quad (5)$$

$$r = \frac{-\varepsilon_{c1}}{\varepsilon_{c2}} \leq 40 \quad (6)$$

4 Results and discussion

4.1 Experimental results

A summary of experimental results of the strengthened and unstrengthened beams is presented in Table 2 and Table 3 respectively. The designation of beam XXY-Z refers to the beam series XX, the beam specimens Y and the number of loaded beam (1 or 2 for PP series and Load or Reload for BC series). The predicted shear resistance V_{CSA} was calculated according to the Canadian standard [7]. This standard is based on the MCFT to define the concrete shear strength V_c and the shear resistance provided by shear reinforcements V_s. The shear strength attributed to concrete is the product between the tensile strength of concrete and a constant β, which is a function of the concrete strain and the crack spacing. The shear resistance attributed to the shear reinforcement is the load which leads to the yielding of the reinforcements that intercepts the main shear crack. For the beam BC3, the overlapping of the shear reinforcements is not considered for the calculation of the steel area A_v. δ_{ult} represents the ultimate deflection at mid-span.

Table 2 Summary of results for the strengthened beams in shear

Beam	V_{exp} [kN]	V_{CSA} [kN]	V_{exp}/V_{CSA}	$V_{c\text{-}CSA}$ [kN]	$V_{s\text{-}CSA}$ [kN]	$V_{s\text{-}exp}$** [kN]	$V_{s\text{-}exp}/V_{s\text{-}CSA}$	δ_{ult} [mm]
PP1-1	476	603	0.79	214	389	262	0.67	13.6
PP2-1	293	420	0.70	243	177	50	0.28	6.7
PP2-2	321	420	0.76	243	177	78	0.44	9.7
PP3-1	504	705	0.71	355	350	149	0.43	12.2
PP3-2	519	705	0.74	355	350	164	0.47	11.4
BC1-L	740	779	0.95	352	427	388	0.91	10.6
BC1-R	801	779	1.02	352	427	448	1.05	39.5
BC2-L	756	783	0.97	357	426	399	0.94	11.9
BC2-R	783	783	1.00	357	426	426	1.00	22.1
BC3-L	956	776	1.23	349	427*	607	1.42	15.5
BC3-R	837	776	1.08	349	427*	488	1.14	37.4
BC4-L	593	796	0.74	362	434	231	0.53	11.5
BC4-R	604	796	0.76	362	434	242	0.56	16.7
BC5-L	731	903	0.81	334	569	397	0.70	12.0
BC5-R	983	903	1.09	334	569	649	1.14	24.3

* This value is calculated with A_v=400mm² ** $V_{s\text{-}exp}=V_{exp}-V_{c\text{-}CSA}$

Table 3 Summary of results for the unstrengthened beams

Beam	V_{exp} [kN]	V_{CSA} [kN]	V_{exp}/V_{CSA}	$V_{strengthened}/V_{unstrengthened}$	δ_{ult} [mm]
PP1-1	329	275	1.19	1.45	7.5
PP1-2	330	275	1.20	-	7.6
PP2-1	283	271	1.04	1.03	6.7
PP2-2	309	271	1.14	1.04	7.6
PP3-1	357	375	0.95	1.41	5.0
PP3-2	355	375	0.95	1.46	4.6

With the results shown in Table 2, it can be observed that the current Canadian standard, as expected, does not adequately predict the shear capacity of beams strengthened with post-installed shear reinforcement. However, Table 3 shows that, with an average V_{exp}/V_{CSA} of 1.08 for the unstrengthened beams, the Canadian standard adequately predict the shear strength of these beams. With a ratio $V_{s\text{-}exp}/V_{s\text{-}CSA}$ between 0.28 and 0.67, the chosen rebar spacing and the anchorage system of strengthened beams PP1, PP2 and PP3 do not allow the development of the yield strength of rebars intercepting shear cracks. By comparing the BC series (BC1 through BC4), it can be seen that the selected strengthening method has a significant impact on the beam shear strength and the involved shear mechanisms. As an example, the expansive mechanical anchorage in beam BC4 has developed only 53% to 56% of the predicted steel strength. This situation is mainly due to the fact that the bars are linked to the concrete section at its top surface and at the expansion anchorage. The deformation of the bars is therefore redistributed across their full length rather than having a local deformation at crack locations which is the case with bonded rebars. The spacing ratio s/d_v has also a significant influence on the shear strength. This phenomenon can be examined with the help of PP3 and BC2 beams respectively. The spacing ratio of 0.75 for the beam PP3 has the effect of allowing main shear cracks to progress near the extremities of the shear reinforcements. The crack location enables the rebars to be properly anchored and to develop their full strength. The selection of a smaller spacing ratio of about 0.6, as for beam BC2, ensures that the rebars are anchored adequately as the main shear cracks intercept these rebars near their mid-length. This can also be observed by comparing the strengthened and unstrengthened beams of the PP series. With a little smaller spacing ratio, the ratio $V_{strengthened}/V_{unstrengthened}$ of the PP1 beams is greater than the PP2 beams. For the selected spacing of the beams PP2, the average of 1.04 means that the shear reinforcements have very small effect on shear strength. As anticipated, the code predictions are in good agreement with the experimental results involving bonded and adequately anchored rebars as it is the case for stirrups for which the code provisions are developed.

4.2 Numerical results and corroboration with experimental tests

For the loading stage of beam BC1, the finite element model and the experiments show a similar behaviour up to about 9.5mm of deflection. At the ultimate shear strength V_{exp} of 740 kN, the deflection δ_{ult} of the beam is 10.6mm, while the FE model predicts a deflection of 15.1mm for an ultimate shear strength of 830kN. For the reloading of the beam BC1, one can observe that the maximum experimental shear strength obtained is 801kN. According to the FE model, the ratios of shear strength V_{FEM}/V_{exp} are 1.12 and 1.04 for the loading and the reloading respectively. The Figure 4 compares the cracking pattern obtained experimentally with the one from the FE model. In a smeared crack model, each finite element (integration point) that reaches the tensile strength will exhibit a crack. However in Figure 4, the cracks with greater openings are illustrated with a bold line. As shown, the path of cracks is very well predicted by the FE model. The crack that leads to shear failure of the beam is the one that passes through the rows of stirrups S3 and S4. With the recorded strain of stirrups well above 23 mm/m, it has been experimentally observed that stirrups S3 and S4 were in the strain hardening behaviour state. The FE model supports this information: at ultimate, the maximum steel stress at the crack are about 493MPa and 481MPa for the stirrups S3 and S4 respectively, which is well above the yield strength of 472MPa.

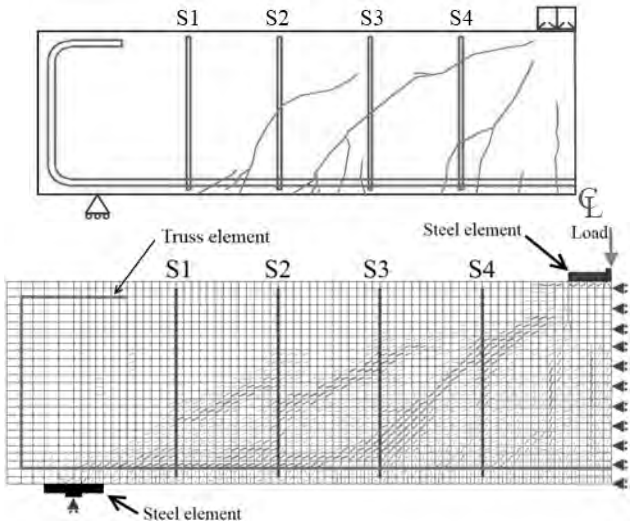

Fig.4 Cracking pattern of the beam BC1 (half beam). Experimental (top) and FE model (bottom)

5 Conclusions and future works

The main goal of this research is to adequately predict the increase of shear strength of thick slabs subjected to various methods of shear strengthening. For the matter, many slab specimens (beams) with different thickness, shear strengthening spacing ratios and strengthening methods were loaded up to failure in the laboratory. While the current Canadian standard is not suited for the shear strength prediction of post-installed shear reinforcements in general, it can nevertheless provide a first good estimate of the ultimate shear strength provided that the rebars are bonded to the section and are adequately anchored up to the beam shear failure which is not the case for all tested beams in Table 2. In this regard, finite element models can provide useful information. Using the VecTor2 software and taking advantage of the symmetry of loading and boundary conditions, half of the beam BC1 was modelled. This beam has been cast with standard stirrups with shear reinforcement spacing well under the maximum spacing ratio permitted by the Canadian code (0.61 versus 0.75).

While the numerical modelling part of the research is still underway, one of the first steps was to be able to replicate the BC1 beam behaviour. By comparing the experimental and numerical results associated to this beam, it appears that its behaviour and its ultimate strength are well evaluated by the model. Moreover, the experimental observations during the loading corroborate the crack pattern predicted by the model and its progression. As mentioned, the cracks' progression and pattern have a major impact on the shear strength of beams, especially those strengthened with rebars link to the concrete section with an epoxy adhesive. Therefore, the next step will be to model this type of shear strengthening and compare the numerical outcomes to the experimental results to perform, thereafter, an in-depth parametric analysis involving the parameters influencing the shear resistance. The testing program has demonstrated that many shear strengthening methods can be used. However, based on practical aspects and effectiveness, the use of additional rebars linked to the concrete section with an epoxy adhesive seems to be promising provided that geometric constrains are satisfied in order for the rebars to remain adequately anchored up to the shear failure.

References

[1] De Lorenzis, L.; Nanni, A.: Shear strengthening of reinforced concrete beams with NSM fiber-reinforced polymer rods. In: ACI structural journal (2001). No. 1, pp. 60-68

[2] Barros, J.A.O.; Dias, S.J.E.: Near surface mounted CFRP laminates for shear strengthening of concrete beams. In: Cement & concrete composites (2006) No. 28, pp. 276-292

[3] Adhikary, B.B.; Mutsuyoshi, H.: Shear strengthening of reinforced concrete beams using various techniques. In: Construction and building materials (2006) No. 20, pp. 366-373

[4] Fernández-Ruiz, M.; Muttoni, A.; Kunz, J.: Strengthening of flat slabs against punching shear using post-installed shear reinforcement. In: ACI structural journal (2010) No. 4, pp. 434-442

[5] Provencher, P.: Renforcement des dalles épaisses en cisaillement (master thesis). In: Département de génie civil, Université Laval, Québec, Canada (2011)

[6] Cusson, B.: Renforcement des dalles épaisses en cisaillement (master thesis). In: Département de génie civil, Université Laval, Québec, Canada (2012)

[7] Canadian Standards Association: Canadian highway bridge design code (2006), 768 p.

[8] Vecchio, F.J.; Collins, M.P.: The modified compression field theory for reinforced concrete elements subjected to shear. In: ACI Journal (1986) No.2, pp. 219-231

[9] Vecchio, F.J.: Disturbed stress field model for reinforced concrete: Formulation. In: Journal of structural engineering (2000) No.9, pp.1070-1077

[10] Lee, S.C., Cho, J.Y, Vecchio, F.J.: Model for post-yield tension stiffening and rebar rupture in concrete members. In: Engineering structures (2011) No.33, pp. 1723-1733

List of symbols

a	Distance between the load and one support
A_s	Area of all tension reinforcement
A_v	Area of all shear reinforcement within a distance *s*
d	Distance from extreme compression fibre to centroid of longitudinal tension reinforcement
d_v	Effective shear deep
f_{c2}	Compressive stress in concrete
h	Height of beam
s	Spacing of transverse reinforcement
V_{exp}	Total shear resistance calculated with experimental data
ε'_c	Concrete compressive strain corresponding to f'_c
ε_{c1}, ε_{c2}	Net concrete axial strain in the principal tensile (1) or compressive (2) direction
ρ	Ratio of tension reinforcement, equal to A_s/bd